Journal of Hydrology (2008) 350, 41–55

available at www.sciencedirect.com

ScienceDirect

journal homepage: www.elsevier.com/locate/jhydrol

Inverse geochemical modeling of groundwater evolution with emphasis on arsenic in the Mississippi River Valley alluvial aquifer, Arkansas (USA)

M.U. Sharif [a,*], R.K. Davis [a], K.F. Steele [a], B. Kim [a], T.M. Kresse [b], J.A. Fazio [c]

[a] Environmental Dynamics Program and Department of Geosciences, University of Arkansas, Fayetteville, AR 72701, USA
[b] U.S. Geological Survey, Water Science Center, 401 Hardin Road, Little Rock, AR 72211, USA
[c] Water Division, Arkansas Department of Environmental Quality, 8001 National Drive, Little Rock, AR 72219, USA

Received 2 June 2007; received in revised form 22 November 2007; accepted 22 November 2007

KEYWORDS
Arsenic;
Hydrogeochemistry;
Inverse modeling;
Saturation indices;
PHREEQC;
MINTEQA2

Summary Inverse geochemical modeling (PHREEQC) was used to identify the evolution of groundwater with emphasis on arsenic (As) release under reducing conditions in the shallow (25–30 m) Mississippi River Valley Alluvial aquifer, Arkansas, USA. The modeling was based on flow paths defined by high-precision (±2 cm) water level contour map; X-ray diffraction (XRD), scanning electron microscopic (SEM), and chemical analysis of boring-sediments for minerals; and detailed chemical analysis of groundwater along the flow paths. Potential phases were constrained using general trends in chemical analyses data of groundwater and sediments, and saturation indices data (MINTEQA2) of minerals in groundwater. Modeling results show that calcite, halite, fluorite, Fe oxyhydroxide, organic matter, H_2S (gas) were dissolving with mole transfers of 1.40E − 03, 2.13E − 04, 4.15E − 06, 1.25E + 01, 3.11, and 9.34, respectively along the dominant flow line. Along the same flow line, FeS, siderite, and vivianite were precipitating with mole transfers of 9.34, 3.11, and 2.64E − 07, respectively. Cation exchange reactions of Ca^{2+} (4.93E − 04 mol) for Na^{+} (2.51E − 04 mol) on exchange sites occurred along the dominant flow line. Gypsum dissolution reactions were dominant over calcite dissolution in some of the flow lines due to the common ion effect. The concentration of As in groundwater ranged from <0.5 to 77 μg/L. Twenty percent total As was complexed with Fe and Mn oxy-hydroxides. The redox environment, chemical data of sediments and groundwater, and the results of inverse geochemical modeling indicate that reductive dissolution of Fe

* Corresponding author. Present address: 60 Clipper Road, Apt. 208, Willowdale, ON, Canada M2J 4E2. Tel.: +1 416 436 3942.
E-mail address: md.sharif@gmail.com (M.U. Sharif).

0022-1694/$ - see front matter
doi:10.1016/j.jhydrol.2007.11.027

oxyhydroxide is the dominant process of As release in the groundwater. The relative rate of reduction of Fe oxyhydroxide over SO_4^{2-} with co-precipitation of As into sulfide is the limiting factor controlling dissolved As in groundwater.

Introduction

Variation in groundwater chemistry is mainly a function of the interaction between the groundwater and the mineral composition of the aquifer materials through which it moves. Hydrogeochemical processes, including dissolution, precipitation, ion-exchange, sorption, and desorption, together with the residence time occurring along the flow path, control the variation in chemical composition of groundwater (Apodaca et al., 2002), that can be modeled by inverse geochemical models. Inverse geochemical modeling is commonly used to reconstruct geochemical evolution of groundwater from one point in an aquifer to another point located in the inverse direction along the groundwater flow path. Recently, inverse geochemical modeling has been used to investigate the chemical evolution of groundwater along the flow path by numerous investigators (Plummer et al., 1990; Rosenthal et al., 1998; Perry, 2001; Eary et al., 2002; Guler and Thyne, 2002; Savage and Bird, 2002; Lakshmanan et al., 2003; Lecomte et al., 2005; Dai et al., 2006; Dhiman and Keshari, 2006; Mirecki, 2006; Clark and Journey, 2006). Inverse geochemical modeling has been also used in several As studies (Schreiber et al., 2000; Carrillo-Chavez et al., 2000; Armienta et al., 2001) to verify if certain geochemical reactions of As release and immobilization are geochemical feasible (Sracek et al., 2004).

Inverse geochemical modeling in PHREEQC (Parkhurst and Appelo, 1999) is based on a geochemical mole-balance model, which calculates the phase mole transfers (the moles of minerals and gases that must enter or leave a solution) to account for the differences in an initial and a final water composition along the flow path in a groundwater system. At least two chemical analyses of groundwater at different points of the flow path, and a set of phases (minerals and/or gases) which potentially react along this flow path are needed to populate the program (Charlton et al., 1997). A number of assumptions are inherent in the application of inverse geochemical modeling: (1) the two groundwater analyses from the initial and final water-wells should represent groundwater that flows along the same flow path, (2) dispersion and diffusion do not significantly affect groundwater chemistry, (3) a chemical steady-state prevails in the groundwater system during the time considered, and (4) the mineral phases used in the inverse calculation are or were present in the aquifer (Zhu and Anderson, 2002). The soundness or validity of the results in the inverse modeling depends on a valid conceptualization of the groundwater system, validity of the basic hydrogeochemical concepts and principles, accuracy of input data into the model, and level of understanding of the geochemical processes in the area (Guler and Thyne, 2004).

One of the most important requirements for inverse model calculation is to prepare an accurate groundwater flow map, which requires a large number of reliable and closely-spaced groundwater elevation data. Measurement of accurate groundwater elevation for a large number of densely spaced wells is a complex, time-consuming and relatively expensive survey technique. The fast static method of surveying (Hofmann-Wollenhof et al., 2001) is most applicable where many points need to be surveyed and the baseline distances are relatively short. This technique generally uses receivers (dual frequency) with code and carrier phase combinations on both frequencies and requires optimum satellite geometry for higher accuracy. This method of surveying technique, which can be used for medium to high accuracy surveys up to 1/1,000,000 for a baseline length up to 100 km (Hofmann-Wollenhof et al., 2001), was applied in the study area.

The natural occurrences of As in groundwater are reported in Bangladesh and West Bengal of India (Bengal Basin), parts of Argentina, Chile, China, Hungary, Mexico, Romania, Taiwan, Vietnam, and many parts of the USA (most commonly in SW of USA) (Smedley and Kinniburgh, 2002). Although, most of these As occurrences include natural sources of enrichment, mining-related sources are also reported. Many new occurrences of high As concentrations in groundwater are being reported in other areas such as parts of Nepal, Myanmar, Cambodia, Ghana, Zimbabwe, South Africa, Australia, and Canada. The most looming threat that As in groundwater can pose is provided in the Ganges—Brahmaputra—Meghna Delta region in Bangladesh (Ahmed et al., 1998, 2004; McArthur et al., 2001, 2004; Nickson et al., 2000; Bhattacharya et al., 2002,2004; Horneman et al., 2004; Zheng et al., 2004, 2005; Harvey et al., 2006). Groundwater has been extensively used as the only source of pathogen-free drinking water in Bangladesh. Unfortunately, the groundwater in Bangladesh is often laden with high As (>50 μg/L, the current MCL for As in Bangladesh) of natural origin. About 50% of the groundwater-wells tested so far exceeded the World Health Organization (WHO) or US EPA's MCL of 10 μg/L of As (BGS and DPHE, 2001). Chronic As poisoning in the As-affected areas in Bangladesh is now widespread and needs immediate measures to provide safe water for at least 20—50 million people (BGS and DPHE, 2001; Smith et al., 2000).

This study is part of a comprehensive research program aimed at characterization of the geochemistry, mobilization, and spatial distribution of arsenic (As) in Jefferson County, southeastern Arkansas, USA. Twenty one of 118 irrigation water wells completed in the shallow (25—30 m thick) Mississippi River Valley alluvial aquifer in the Bayou Bartholomew watershed, southeastern Arkansas had As concentrations (<0.5—77 μg/L) exceeding 10 μg/L (Kresse and Fazio, 2003; Sharif, 2007). Hydrogeochemical data and redox environment in the area suggest reductive dissolution of Fe oxyhydroxide as the dominant As release mechanism (Kresse and Fazio, 2003; Sharif, 2007).

In this paper, physical, hydrogeologic, and hydrogeochemical information from the groundwater and aquifer sediments were incorporated into the inverse geochemical modeling to determine the flow path evolution of groundwater, and its

relation to the mobilization of As in groundwater within the aquifer.

Study area

Location

The study area is about 225 km^2 in the southern part of Jefferson County, Arkansas (Fig. 1). It is bounded by the Arkansas River to the northeast and Bayou Bartholomew to the southwest. The area comprises the northeastern part of the Bayou Bartholomew watershed, which is covered almost entirely by Holocene alluvial deposits of the Mississippi and Arkansas rivers. Row-crop agriculture represents the major land use in the floodplain, whereas silviculture dominates the land use in the terrace portion of the watershed. Eastern Arkansas receives an annual precipitation of 1.2—1.4 m (Freiwald, 1985). Reliance on water from the alluvial aquifer for crop production has increased dramatically over recent years. The increase in estimated

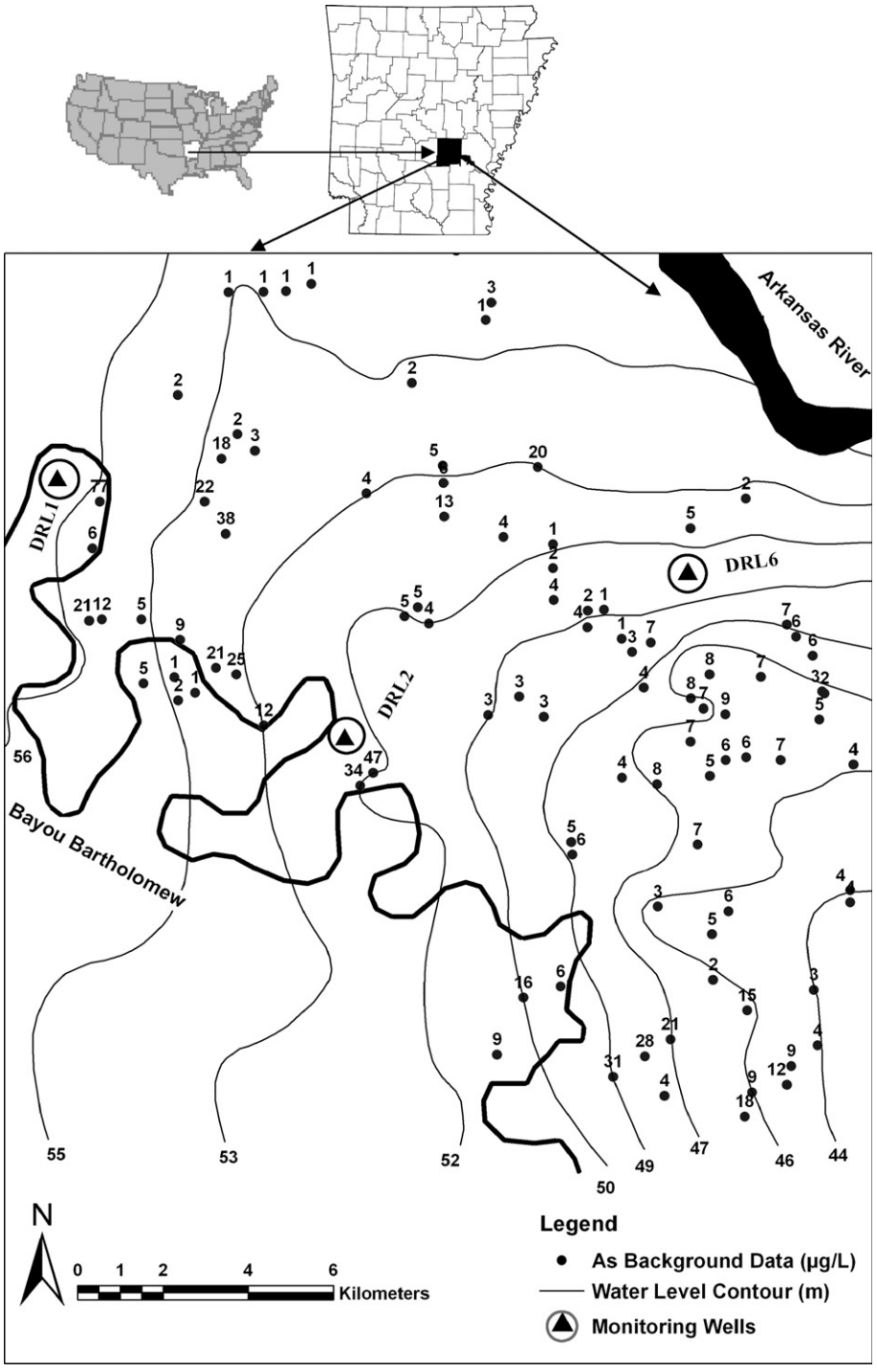

Figure 1 Map showing location of study area, nested monitoring wells sites, water level map, and As background data.

groundwater withdrawals from 1985 to 1995 was about 45% (Schrader, 2001).

Hydrogeologic settings

The Holocene alluvial deposits in the research area are represented by fining upward sequences from gravels and coarse sands at the base to fine sands, silts, and clays at the surface (herein referred to as surface aquitard). Pleistocene alluvial deposits of the Mississippi and Arkansas rivers form terraces with minor exposures of Tertiary-age strata along topographically high areas, and are found beyond the western part of the study area (Kresse and Fazio, 2002). The thickness of the surface aquitard varies from <6 to 12 m, and permeability of the aquitard is heterogeneous due to varying proportions of clay, silt, and fine sands. Where the surface aquitard is thick and less permeable, it forms a confining unit which impedes recharge to the alluvial aquifer. The thickness of the alluvial aquifer ranges from 18 to 43 m (Kleiss et al., 2000). Channel fill, point bar, and back swamp deposits associated with present and former channels of the Mississippi and Arkansas rivers produced abrupt changes in lithology and resulted in large spatial and vertical variations in the hydraulic properties of aquifer system (Joseph, 1999). The regional direction of groundwater flow is generally to the south and east except where affected by intense groundwater withdrawals (Schrader, 2001). Local perturbations in flow directions result from the influent–effluent character of smaller streams within the study area.

Materials and methods

Monitoring wells

Collection of cuttings

Within the 225 km^2 study area three contrasting sites for nested monitoring wells were selected as a high As (>50 μg/L) area in the northwest (DRL1), a medium As (10–50 μg/L) area in the south (DRL2), and a low As (<10 μg/L) area in the northeast (DRL6). These locations for monitoring wells were selected based on As background data (Kresse and Fazio, 2002), geologic cross-sections prepared from borehole logs of Arkansas Geologic Commission (AGC), groundwater flow maps, distribution of surface aquitard, and primary recharge areas. Three pairs of nested monitoring wells were drilled, installed, developed, and sampled at the selected sites in February 2006.

A hollow stem auger drill rig equipped with a 152 cm long and 7.62 cm outside diameter (O.D.) CME® sampler (steel) was used to extract continuous sediment cores to a depth of 12 m. The same rig equipped with a 46 cm, split-spoon sampler accepting a 5 cm O.D. steel liner was used to collect cores at approximately 150 cm intervals to a depth of 36.5 m. No drilling fluid was used to minimize borehole contamination. Core recovery using the CME® sampler was 80% or greater, while a varying rate of 30–90% core recovery was achieved with the split-spoon sampler. The lower-volume core recovery was due to the increase of fine sand fractions which flowed from the core barrel even with the use of sediment traps. The extracted cores were collected, wrapped in aluminum foil, labeled, and transported to the laboratory for physical and chemical analysis. A sub-sample (about 200 g) of each core was also separated in the field into plastic Ziploc® bags, and preserved below 4 °C to provide fresh sample for Fe speciation, and comparison between extraction procedures using dry and fresh wet sediments. Sediment samples were labeled numerically after the monitoring well ID (e.g. DRL1S1, DRL1S2).

Installation of monitoring wells

At each site two monitoring wells with 5 cm O.D. PVC pipe were installed at a depth of 10.6 and 36.5 m, respectively. The shallow wells were screened from 4.6 to 10.6 m and the deep wells were screened from 33.5 to 36.5 m. Each aspect of monitoring well installation was completed by standard procedures (Wayne et al., 1997) and complied with federal, state, and local regulations. The depth to groundwater was measured with a Solinst® Model 101 meter. Accurate groundwater elevation was calculated from post-processed land-surface elevation data (with an estimated precision of ±2 cm) generated by survey-grade Trimble® 4000SSE GPS units using the Fast Static method of data collection. The monitoring wells were initially developed using a PVC bailer attached to the wire-line on the drill rig, and secondarily using a Redi-Flo® VFD GRUNDFOS pump.

Groundwater sampling, field Monitoring, and laboratory analyses

All chemical analyses were performed on groundwater samples collected from the monitoring wells with a generator-driven submersible pump (Redi-Flo® VFD GRUNDFOS) in June 2006. Sample collection, handling, and preservation procedures of United States Geological Survey (Shelton and Chapel, 1994) were followed to ensure data quality and consistency. Prior to sample collection, the well was pumped continuously for 30–45 min until the temperature, electrical conductance (EC), pH, oxidation reduction potential (ORP), and dissolved oxygen (DO) readings stabilized within the accepted guidelines of NAWQA. After recording readings of these stabilized monitoring parameters, a number of other redox sensitive chemical parameters including Fe and As speciation, Mn^{2+}, and dissolved S^{2-} were measured by standard methods (Clesceri et al., 1999) in the field (Table 1). Volatile organic and inorganic compounds were measured at the well head by EPA method 21 (U.S. EPA, 1999). Chemical data are given in Table 2.

Collection of groundwater samples for total analyses

A set of four groundwater samples were collected in 100 mL HDPE bottles that were (1) filtered (0.45 μm) and acidified, (2) not-filtered and acidified, (3) filtered (0.20 μm) and acidified, and (4) filtered (0.45 μm) and not-acidified. Acidification was achieved by adding concentrated HNO_3 (VWR® Omni trace grade) until pH reached 2 or less standard units. Dissolved cations including Ca^{2+}, Mg^{2+}, Na^{+}, K^{+}, SiO_2, Mn^{2+}, Fe^{2+}, Al^{3+}, Ag, B, Ba, Be, Cd, Cr, Cu, Li, Ni, Mo, Pb, Se, Sb, Sr, Ti, Zn, V, and As were measured on the acidified samples by Inductively Coupled Plasma-Mass Spectrometer (ICP-MS) following EPA method 200.8 (U.S. EPA, 1994). Dissolved anions including Cl^{-}, Br^{-}, F^{-}, SO_4^{2-}, NH_4-N, NO_3^{-}–N, PO_4^{3-}–P were measured on the non-acidified samples by Ion Chromatograph following standard EPA method Anion

Table 1 Groundwater quality data including redox-sensitive chemical parameters were measured by standard methods (Clesceri et al., 1999) at three sites of nested monitoring wells

Parameters	Units	Instrument and model	Methods
Temperature	°C	YSI® Model 30 handheld	
EC	μS/cm	Salinity, Conductance, and Temperature Meter	
pH		Multi Probe Orion® 3-Star portable pH/ORP meter	
ORP	RmV		
Dissolved oxygen (DO)	mg/L	YSI® 550A Dissolved Oxygen Meter	
Alkalinity	mg/L as $CaCO_3$	HACH® Digital Titrator	Sulfuric acid titration
Dissolved S^{2-}	μg/L	HACH® spectrophotometer (DR 2800)	Methylene Blue
Fe^{2+}	mg/L		1, 10 Phenanthroline
Fe (total)	mg/L		FerroVer
Mn^{2+}	mg/L		Periodate Oxidation
Inorganic As speciation	μg/L	Separated using anion exchange columns and measured by ICP-MS	Edwards et al., 1998
Inorganic and organic As speciation	μg/L	Separated using anion and cation exchange columns and measured by ICP-MS	Grabinski, 1981
Volatile organic and inorganic compound (methane, benzene, hexane, ammonia, hydrogen sulfide, carbon tetrachloride, etc.)	ppm	Thermo® TVA-100B Toxic Vapor Analyzer, which uses both Flame Ionization Detector (FID) and Photo Ionization Detector (PID)	EPA method 21 (USEPA, 1999)

300.0 (Pfaff, 1993). TOC was measured by a TOC analyzer using the liquid sample module. Chemical data including redox sensitive chemical parameters are given in Table 2. Filtering was done using two disposable syringes with filters (0.45 and 0.20 μm). Both filtered and non-filtered samples were analyzed by ICP-MS to identify the significance of particulate trace metals (e.g. As, Fe) in groundwater. All groundwater samples were analyzed in the Arkansas Department of Environmental Quality (ADEQ) laboratory, Little Rock, AR. Standard calibrations were based on standard addition for all dissolved ions analyzed in the laboratory.

Preparation of sediment samples and laboratory analyses

Sealed sections of the stored core samples were opened and sub-sampled in February 2006 for grain size, porosity, and geochemical analyses. About 100 g of stored sediment from each core were separated and dried below 40 °C in an oven. The sediments were crushed by a conventional porcelain pestle and mortar, and passed through a 1 mm nylon screen. These screened sediment samples were used for a sequential extraction procedure for major cations and trace metals, including As. Grain-size analysis was done with little or no crushing on dried pre-screened samples by using a micro pipette method (Miller and Miller, 1987). Porosity was measured by weighing 50 mL hand-packed sediments in a graduated cylinder. Water was slowly added to the 50 mL mark and the sample was shaken to remove air bubbles and saturate evenly with water. Gravimetric porosity $[(1 - \rho^b/\rho_s)]$ was calculated by mean particle density (ρ_s = mass of solids/volume of solids) and dry bulk density (ρ_b = mass of dry solids/volume of dry solids). The five-step sequential extraction (modified from Tessier et al., 1979 and Chao and Zhou, 1983) was conducted using 2 g dry sediment. The steps of the extraction procedures are as follows:

1. Exchangeable: 16 mL of 1 M sodium acetate to pH 8.2 for 1 h.
2. Carbonates: 16 mL of 1 M sodium acetate to pH 5 for 4 h.
3. Amorphous Fe and Mn oxides: 40 mL of 0.25 M NH_2—OH—HCl (hydroxylamine hydrochloride) in 0.25 M HCl; heat to 50 °C for 30 min.
4. Organic matter: 6 mL of 0.02 M HNO_3 and 10 mL of 30% H_2O_2 to pH 2 with HNO_3; heat to 85 °C for 2 h, and later 6 mL of 30% H_2O_2; heat to 85 °C for 3 h.
5. Hot HNO_3 leachable As: 15 mL of 7 M HNO_3 for 2.5 h at 70 °C for the first 30 min and later at 100 °C for the next 2 h.

The last step of the sequential extraction (hot HNO_3 extraction) was used to represent the least environmentally-available As. A separate rigorous HNO_3—H_2SO_4 acid leachable (9 mL concentrated HNO_3, 4 mL concentrated H_2SO_4, and 5 mL distilled deionized water was added in the digestion tube with 2 g dry sediment to heat at 90 °C for 30 min) extraction (Adeloju et al., 1994) were also completed. A total of 60 sediment samples were extracted. Sediment extraction data are listed in Table 3. Five duplicates, one gravel-pack sample, a bentonite grout sample, eight wet sediment samples preserved in the freezer, and two coarse (>1 mm) sediment samples were also extracted for quality control and comparison purposes. The extracted solutions were shipped to the ADEQ laboratory in Little Rock, Arkansas for analysis by ICP-MS.

XRD and SEM analyses

Thirty dried sediment samples were powdered using a grinding mill (RockLabs®) for X-ray Diffractometry (XRD) and Scanning Electron Microscopic (SEM) analysis. XRD

Table 2 Chemical data for groundwater in the monitoring wells

Parameter	DRL1S	DRL1D	DRL2S	DRL2D	DRL6S	DRL6D
Water level (m bls)	5.6	5.7	6.9	6.8	8.4	8.3
Temperature (°C)	18.5	17.9	19.5	18.5	18.9	18.5
EC (μS/cm)	310	306	456	426	953	658
TDS (mg/L)	209	187	261	241	572	382
pH	6.11	6.13	6.87	6.81	6.84	6.68
Alkalinity (mg/L as $CaCO_3$)	108	135	215	189	437	300
ORP (RmV)	198	124	55	66	−247	−223
DO (mg/L)	0.4	0.08	0.06	0.06	0.08	0.08
Hardness (mg/L)	102	61	177	164	426	278
Total dissolved As (μg/L)	0.73	29.6	12.3	39.7	49.4	1.02
As(III) (μg/L)	<0.5	10.2	1.14	8.22	5.23	<0.5
As(V) (μg/L)	0.7	20.3	11.4	33.9	45.3	1.15
Particulate As (μg/L)	0.1	0	0	2.2	0	0.3
Total Fe (mg/L)	1.9	41	11.5	16.3	8.3	11
Fe^{2+} (mg/L)	0.04	9.2	7.3	8.5	4.6	5.8
Fe^{3+} (mg/L)	1.6	31.8	4.2	7.8	2.8	3.9
Particulate Fe (mg/L)	0.24	1.7	0.1	0	0.16	0.3
Ca^{2+} (mg/L)	25.4	17.4	55.6	48.8	130	80
Mg^{2+} (mg/L)	9.3	4.4	9.4	10.3	24.7	18.9
Na^{+} (mg/L)	16.3	11.7	16.3	17.1	41.8	18.7
K^{+} (mg/L)	2	2.6	1.1	1.4	1.5	1.2
Mn^{2+} (mg/L)	2.7	1.5	0.5	0.7	0.4	0.7
Cl^{-} (mg/L)	14.2	20.1	7.7	7.6	27.1	29.6
SO_4^{2-} (mg/L)	18	2	1	1.4	46	1.4
NO_3^{-}—N (mg/L)	2.25	<0.01	<0.01	<0.01	<0.01	<0.01
NH_4—N (mg/L)	0.03	0.21	0.9	0.35	1.1	0.72
PO_4—P (mg/L)	0.02	0.03	0.03	0.05	0.02	0.05
S^{2-} (μg/L)	2	6	11	51	27	27
SiO_2 (mg/L)	31.7	32.9	31.6	34	34.4	28.3
Br^{-} (mg/L)	0.08	0.08	0.06	0.06	0.14	0.12
Ba^{2+} (μg/L)	166	198	215	150	538	388
B^{3+} (μg/L)	25	13	35	30	42	44
Fl^{-} (mg/L)	0.4	0.3	0.3	0.4	<0.01	0.3
Zn^{2+} (μg/L)	2.7	5.2	2.4	3.8	1.7	1.4
V^{5+} (μg/L)	0.96	0.51	<0.50	<0.50	<0.50	<0.50
Co^{2+} (μg/L)	1.95	6.44	0.52	<0.50	<0.50	<0.50
Ni^{2+} (μg/L)	2.7	4.4	<0.50	<0.50	<0.50	<0.50
TOC (mg/L)	6.2	6.8	6	6.3	11	6.8
Volatile organic and inorganic compound (ppm)	<0.1	<0.1	0.3	0.5	1.4	0.7

measurements used Cu Kα radiation and a graphite monochrometer on a Philips® vertical diffractometer, stepped at 0.5 s/0.02°, from 2° to 100° 2θ. Iterative identification of minerals in the samples used PC-APD® Diffraction software of Philips Analytical with search/match of the reference mineral database and generated powder patterns. Five sediment samples were magnetically separated by a Frantz® Isodynamic Separator Model L-1 and were analyzed by XRD. A subset of the magnetically separated minerals was analyzed by a Hitachi® S-2300 SEM to identify the nature of crystallinity of magnetic minerals.

Organic carbon and inorganic sediment sulfur analyses

Thirty sediment samples from three monitoring well sites were analyzed for total organic carbon (TOC) and inorganic sediment sulfur. TOC was analyzed using a Shimadzu® TOC 5050 analyzer equipped with the solid sample module (SSM 5000A). Reduced inorganic sulfur compounds (pyrite + elemental sulfur + acid volatile monosulfides) were measured by the chromium reduction method or Canfield method (Canfield et al., 1986). Chromium reduction does not reduce or liberate either organic sulfur or sulfate sulfur, which makes the method specific only to reduced inorganic sulfur phases. The detection limits for TOC and inorganic sediment sulfur were 0.1% and 0.01% of sediment, respectively. Table 4 shows the results of TOC and reduced sediment sulfur in the sediments.

Groundwater quality data from irrigation wells

Groundwater quality data (Table 5) were obtained from existing irrigation wells (Kresse and Fazio, 2002) in the research area. The wells ranged in depth from approximately 24—49 m. Groundwater samples were collected from as

Table 3 As concentration (mg/kg) from Tessier's sequential extraction and a separate single extraction of hot HNO_3 and H_2SO_4

Depth (m)	Lithology	Exchangeable	Carbonates	Amorphous Fe + Mn oxide	Organic	Hot HNO_3	Extraction total	Hot HNO_3 and H_2SO_4
DRL1								
0	Sandy Silt	<0.037	0.31	0.47	0.22	0.75	1.44	1.59
0.3	Silty Sand	0.05	<0.37	5.98	5.25	4.45	16.7	18.1
0.6	Silty Sand	<0.037	<0.37	0.45	0.16	1.11	1.73	2.10
2.1	Clayey Silt	<0.037	<0.37	0.38	0.13	2.09	2.60	2.95
3	Clayey Silt	<0.037	<0.37	0.41	0.15	1.83	2.39	3.01
4.9	Sandy Silt	<0.037	<0.37	0.53	<0.12	1.07	1.60	3.18
6.1	Clayey Silt	<0.037	<0.37	0.68	<0.12	1.74	2.42	2.38
7	Clayey Silt	<0.037	<0.37	0.57	<0.12	2.88	3.44	2.63
7.6	Silty Sand	<0.037	<0.37	0.25	<0.12	0.79	1.04	4.10
8.8	Sand	<0.037	<0.37	0.52	<0.12	1.62	2.18	1.97
10.1	Sand	<0.037	<0.37	0.24	<0.12	0.78	1.02	2.09
13.7	Sand	<0.037	<0.37	<0.12	<0.12	0.23	0.23	<0.5
16.8	Sand	<0.037	<0.37	0.13	<0.12	0.25	0.37	<0.5
18.3	Sand	<0.037	<0.37	0.46	<0.12	1.04	1.50	<0.5
21.3	Clay Lens	<0.037	<0.37	0.50	<0.12	4.55	5.05	0.79
24.4	Sand	<0.037	<0.37	<0.12	<0.12	0.14	0.14	4.33
25.9	Sand	<0.037	<0.37	0.21	<0.12	0.31	0.51	<0.5
33.5	Sand	<0.037	<0.37	0.14	<0.12	0.36	0.50	<0.5
36.4	Sand	<0.037	<0.37	0.17	<0.12	1.15	1.32	<0.5
36.6	Clay Lens	<0.037	<0.37	1.10	<0.12	3.38	4.55	1.35
DRL2								
0.0	Silt	0.07	<0.37	0.99	<0.12	1.99	3.05	3.35
0.8	Sandy Silt	<0.037	<0.37	0.44	<0.12	1.91	2.59	2.58
1.5	Clayey Silt	<0.037	<0.37	0.49	<0.12	2.10	3.99	3.68
2.4	Sandy Silt	<0.037	<0.37	0.99	<0.12	3.40	2.35	3.15
4.0	Clayey Silt	<0.037	<0.37	1.14	<0.12	2.85	4.39	3.78
5.5	Sandy Silt	0.06	<0.37	0.46	<0.12	1.59	2.11	2.58
6.4	Clayey Silt	<0.037	<0.37	0.61	<0.12	2.58	3.19	1.67
7.6	Silt	<0.037	<0.37	0.56	<0.12	1.72	2.28	1.53
9.1	Sand	<0.037	<0.37	<0.12	<0.12	0.27	0.27	<0.5
10.7	Sand	<0.037	<0.37	0.65	<0.12	3.60	4.25	1.80
12.2	Sand	<0.037	<0.37	<0.12	<0.12	0.27	0.27	<0.5
13.7	Clayey Silt	<0.037	<0.37	<0.12	<0.12	0.13	0.13	<0.5
15.2	Sand	<0.037	<0.37	<0.12	<0.12	0.13	0.13	<0.5
18.3	Clay	<0.037	<0.37	0.59	<0.12	1.37	1.96	0.79
21.3	Sand	0.05	<0.37	0.37	<0.12	1.00	1.42	0.70
30.5	Sand	<0.037	<0.37	0.12	<0.12	0.20	0.20	<0.5
DRL6								
0.0	Sandy Silt	0.07	<0.37	0.28	<0.12	1.92	2.27	2.42
0.6	Silt	<0.037	<0.37	0.28	<0.12	1.79	2.07	2.10
1.1	Clayey Silt	0.08	<0.37	1.45	<0.12	5.45	6.98	4.43
5.5	Sandy Silt	<0.037	<0.37	0.27	<0.12	0.47	0.74	<0.5
7.3	Clayey Silt	<0.037	<0.37	2.22	<0.12	3.53	5.75	2.38
8.2	Silty Clay	0.04	<0.37	0.84	<0.12	1.92	2.80	1.14
10.4	Clayey Sand	<0.037	<0.37	0.43	<0.12	0.70	1.12	0.56
10.7	Clayey Sand	<0.037	<0.37	0.33	<0.12	0.86	1.19	0.56
11.0	Silty Sand	<0.037	<0.37	0.21	<0.12	0.46	0.67	<0.5
12.2	Silty Sand	0.04	<0.37	5.10	<0.12	22.8	27.9	9.30
12.8	Sand	<0.037	<0.37	2.02	<0.12	2.40	4.42	2.63
15.2	Sand	<0.037	<0.37	0.25	<0.12	0.61	0.86	0.68
24.4	Sand	<0.037	<0.37	0.64	<0.12	1.83	2.46	1.51
27.4	Sand	<0.037	<0.37	0.17	<0.12	0.45	0.62	<0.5
30.5	Sand	0.06	<0.37	0.26	<0.12	0.90	1.22	0.94
36.6	Sand	0.06	<0.37	0.24	<0.12	0.79	1.09	0.91

Table 4 Total organic carbon and reduced inorganic sulfur analyses results

Lithology	Depth (m)	*TC (%)	*TIC (%)	*TOC (%)	*IS (%)	Remarks
Sandy Silt	0	ND	ND	ND	*ND	No sediment sulfide is detected
Clayey Silt	1.1	1.20	1.04	0.16	*ND	above the water table
Sandy Silt	5.8	0.18	<0.1	<0.1	*ND	
Clayey Sand	7.3	0.97	0.16	0.81	0.043	
Silty Clay	8.2	0.84	0.12	0.72	<0.01	
Clayey Sand	10.1	0.18	ND	0.18	*ND	
Silty Sand	11	<0.1	ND	<0.1	*ND	
Sand	12.8	<0.1	ND	<0.1	0.032	
Clay Lens	24.4	0.17	ND	0.17	<0.01	
Sand	36.6	<0.1	ND	<0.1	<0.01	
Silt	0.1	0.43	ND	0.43	ND	Sediment sulfide is present
Clayey Silt	1.5	0.11	<0.1	0.11	ND	below the water table
Clayey Silt	6.4	0.16	ND	0.16	ND	
Silty Sand	6.7	<0.1	ND	<0.1	ND	
Silt	7.6	0.24	ND	0.24	ND	
Sand	10.7	0.67	ND	0.67	0.047	
Sand	12.2	<0.1	ND	<0.1	ND	
Sand	21	0.28	ND	0.28	<0.01	
Sand	21.3	<0.1	ND	<0.1	<0.01	
Sandy Silt	0.1	0.17	ND	0.17	ND	Significant sediment sulfide is
Clayey Silt	2.1	0.17	ND	0.17	ND	also present in sands at depths
Clayey Silt	3	0.20	ND	0.20	ND	
Sandy Silt	4.9	<0.1	ND	<0.1	ND	
Clayey Silt	6.1	0.10	ND	0.10	ND	
Sandy Silt	6.4	<0.1	ND	<0.1	ND	
Sand	10.2	<0.1	ND	<0.1	ND	
Sand	18.3	<0.1	ND	<0.1	<0.01	
Clay Lens	18.6	<0.1	ND	<0.1	0.016	
Sand	33.5	ND	ND	ND	ND	
Clay Lens	36.6	0.76	ND	0.76	0.11	

*ND, not detected.
*TC, total carbon, TOC analyzer, detection limit: 0.1%.
*IC, inorganic carbon, TOC analyzer, detection limit: 0.1%.
*IS, inorganic sulfide, Canfield method, detection limit: 0.01%.

near to the wellhead as possible and delivered to the ADEQ laboratory for analysis of major ions and trace metals. Groundwater samples were labeled numerically after the initials ''JF'' for Jefferson County of Arkansas. Groundwater samples for analysis of metals were filtered through a 0.45 μm pore-sized membrane and preserved with nitric acid to a pH of 2.0. Trace metals, including As, were run on a plasma optical-emission mass spectrometer by EPA method 200.8. Analysis of temperature, pH, and conductance was performed in the field at the time of sampling with an Orion[tm] multifunction portable meter.

The water quality data were lacking several important redox-sensitive parameters, including Fe and As speciation, dissolved oxygen (DO), dissolved hydrogen sulfide, and oxidation reduction potential (ORP). In order to supplement the necessary geochemical parameters, including redox-sensitive chemical parameters (DO, ORP, As and Fe speciation data, dissolved hydrogen sulfide, volatile organic carbon), groundwater quality data generated from three pairs of nested monitoring wells (10 and 36 m deep) in the research area are considered.

Groundwater flow path

Survey-grade GPS (Trimble® 4000SSE) with a fast static method of data collection was used with one control receiver placed over a known control point, usually in the middle of the survey area. A rover or remote receiver was used at each unknown station (here irrigation-well site) for 5–20 min to collect survey data depending on the baseline length, the number of visible satellites, the geometric configuration, and the method used. Two GPS receivers were used to measure a GPS baseline vector. The line between a pair of GPS receivers from which simultaneous GPS data were collected and processed was a vector referred to as a baseline (Hofmann-Wollenhof et al., 2001).

The collected GPS data were post-processed to increase the positional accuracy of the surveyed site. The Trimble Geomatics Office software v. 1.62 provided the ability to generate post-processed GPS baseline solutions when the baseline processor module (BPM) was installed. The BPM used the weighted ambiguity vector estimator (WAVE) for baseline solutions. This program was used to compute

Table 5 General statistics of the chemical data of irrigation water wells used for groundwater quality monitoring in the area (Kresse and Fazio, 2002)

Parameters measured	Minimum	Maximum	Mean	Median	Std. deviation
Water level (m)	3.3	12.4	7.4	7	2.16
Temperature (°C)	17.3	19.5	17.9	18	0.47
Conductivity (μS/cm)	148	1353	528	421	309
TDS (mg/L)	168	746	327	261	157
pH	6.11	7.06	6.7	6.8	0.24
Alkalinity (mg/L as $CaCO_3$)	52	437	219	188	111
Hardness (mg/L)	43	491	203	164	127
As (μg/L)	0.73	50	14.1	7	15.3
Fe (mg/L)	1.87	41	11.9	10.5	8.1
Ca (mg/L)	10.6	143	58.7	48.6	37.6
Mg (mg/L)	4.1	33.5	13.8	10.3	8.3
Na (mg/L)	10.7	72	25.1	18.7	15.1
K (mg/L)	0.46	4.9	1.96	1.9	1.05
Mn (mg/L)	0.29	1.8	0.68	0.6	0.37
Cl (mg/L)	4.82	116	25.5	18	27.9
SO_4 (mg/L)	0.95	85.2	12.2	4	19.1
NO_3—N (mg/L)	<0.01	2.25	0.14	0.02	0.43
NH_3—N (mg/L)	0.04	1.06	0.29	0.23	0.25
PO_4—P (mg/L)	<0.005	0.1	0.03	0.02	0.03
Ni (μg/L)	<0.5	4.4	1.9	2	0.75
Cu (μg/L)	<5	46	7.2	5	7.8
SiO_2 (mg/L)	24.7	51.7	33.5	32.3	4.8
Br (mg/L)	<0.01	0.52	0.12	0.09	0.12
Ba (μg/L)	0.12	0.78	0.27	0.14	0.17
B (μg/L)	4.5	48.6	18.5	13.4	14.7
F (mg/L)	<0.01	0.4	0.24	0.23	0.08
Zn (μg/L)	<1	5	1.8	1.7	1
V (μg/L)	<0.5	1.9	1	1	0.33
Cr (μg/L)	<0.4	3	0.7	0.5	6.6
TOC (mg/L)	0.33	11	2.8	1.8	2.5

baseline solutions from GPS field observations made using the fast static method of data collection. The baseline processor used both carrier phase and code observations to produce three-dimensional GPS baselines between survey points. The station coordinate differences were calculated in terms of a 3D, earth-centered coordinate system that utilized X, Y, and Z values based on the WGS 84 geocentric ellipsoid model. The vertical accuracy of fast static surveys was two centimeters or less.

The depth to groundwater was measured with a Solinst® Model 101 water-level meter. Accurate groundwater elevation for each irrigation well site was calculated from the measured water level and the post-processed, land-surface elevation data for the same irrigation well site. The post-processed groundwater elevation data from 174 irrigation water wells in Jefferson County, Arkansas, were used to prepare a detailed high-precision groundwater flow map. Groundwater flow vectors and modeled flow lines are shown on the groundwater flow map (Fig. 2).

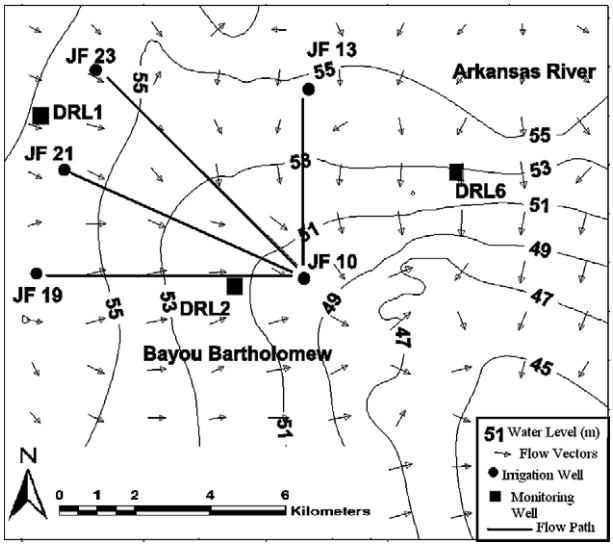

Figure 2 Groundwater flow vectors and modeled flow lines with irrigation water wells (solid circles) and nested monitoring wells (solid squares) in the study area.

Inverse geochemical modeling

The USGS geochemical code PHREEQC (Parkhurst and Appelo, 1999) was used for inverse geochemical modeling. General flow direction from a high-precision water level contour map was used to select initial and final locations for groundwater quality wells. Due to better spatial

coverage with respect to groundwater flow paths in the area, groundwater quality data of irrigation wells were used in the inverse geochemical models. The model was run along four predefined flow lines (JF19—JF10, JF21—JF10, JF23—JF10, and JF13—JF10) moving down gradient. Potential phases (minerals) for the model run were selected from XRD, SEM, and chemical analysis of sediment samples. Potential phases in the inverse modeling were constrained (precipitation/dissolution) using a conceptual model of general trends in chemical data and saturation indices (logarithm of the quotient of the ion activity product (IAP) and solubility product constant (K_{SP})) data (over-saturated phases were allowed to precipitate) of groundwater of selected water-wells (Table 6) derived from MINTEQA2 (Allison et al., 1991).

The inverse modeling in PHREEQC takes into account uncertainty limits that are constrained to satisfy the mole balance for each element and valance state, as well as the charge balance for each solution within the simulation. The simulations were constrained within the specified uncertainty limit, which were selected as 0.025 or 0.05 as default for all model runs. The models were first run using the ''Minimal'' identifier. After checking for adequacy and geochemical consistency, the models were rerun using ''Multiple Precision Solver'' (with a default tolerance of $1E-12$) without the ''Minimal'' identifier for details. A set of uncertainty terms is generated for each inverse model by the PHREEQC program to account for uncertainties in the model simulation: (1) the sum of residuals is the sum of the uncertainty of the unknowns weighted by the inverse of the uncertainty limit (for this application it is <8), (2) the sum of delta/uncertainty is the sum of the adjustments to each element concentration weighted by the inverse of the uncertainty limit (for this application it is <8), and (3) maximum fractional error in element concentration is the adjustment to any element concentration in any solution (for this application it is <0.07). If no adjustments are made, all three quantities would be zero.

Results

Sediment geochemistry

The qualitative identification of XRD detects quartz, orthoclase feldspar, calcite, dolomite, gypsum, fluorite, goethite, hematite, magnetite, kaolinite, smectite, illite, and chlorite as crystalline phases in the sediment samples. No pure As mineral phases (e.g. realgar, orpiment, arsenopyrite) were identified by XRD and SEM analysis. SEM analyses of magnetic minerals revealed a mix of well crystalline, poorly crystalline (semi/sub-crystalline), and amorphous phases. The amorphous magnetic phases are assumed to be ferrihydrite, the most common Fe oxyhydroxide in sedimentary environments. Amorphous Fe oxyhydroxide phases were also quantified by chemical extraction step of Tessier's five-step sequential extraction procedures using Chao reagent (Tessier et al., 1979; Chao and Zhou, 1983), which dissolves amorphous phases of Fe and Mn oxyhydroxides. The extraction step using Chao reagent of the Tessier's sequential extraction procedure is well reported in the scientific community (Rodriguez et al., 2003; Miller, 2001; Chao and Zhou, 1983) for determining amorphous metal oxide surface population. Specifically, Fe concentrations in sediment extracts extracted by Chao reagent are used to back-calculate (using molecular ratio of Fe/amorphous Fe oxyhydroxide) the amount of amorphous Fe oxyhydroxide that was present on the sediment grains as coatings (Dzombak and Morel, 1990; Parkhurst and Appelo, 1999). Sequen-

Table 6 Saturation indices (MINTEQA2) data showing supersaturated phases (super-saturated phases are allowed to precipitate that present as finite solids) and undersaturated phases in groundwater

Phases	JF10	JF13	JF19	JF21	JF23
Sphalerite	−4.46	Supersaturated	−5.49	Supersaturated	−5.40
FeS (ppt)	−9.85	−2.29	−11.1	−2.65	−7.86
Ferrihydrite	−6.01	−6.01	−5.22	−5.78	−6.14
Goethite	−3.26	−3.25	−2.45	−3.02	−3.80
Hematite	−4.15	−4.14	−2.54	3.67	−4.39
Siderite	−0.29	Supersaturated	Supersaturated	−0.60	Supersaturated
Fluorite	−1.91	−1.60	−2.80	−2.25	−2.05
Halite	−8.26	−8.08	−8.06	−8.40	−8.26
Calcite	−0.58	−0.05	−0.40	−1.33	−0.92
Dolomite	−1.49	−0.47	−1.20	−2.94	−2.31
Gypsum	−3.25	−2.23	−3.30	−2.96	−2.92
Barite	−0.80	Supersaturated	−0.38	−0.28	−0.49
Manganite	−8.92	—	−9.83	—	−8.14
Magnesite	−1.84	−1.34	−1.72	−2.54	−2.34
Vivianite	−4.84	−5.97	−5.56	−5.01	−2.78
$FeAsO_4 \cdot 2H_2O$	−19.0	−19.0	−16.3	−17.7	−18.4

Groundwater in all the wells is supersaturated with quartz, magnetite, pyrite, and $Ba_3(AsO_4)_2$

Saturation index (SI) = log [Ion activity product (IAP)]/[Equilibrium constant (*KT*) at temperature *T*. Phases are constrained to be present either super-saturated or under-saturated. Saturation indices were calculated by the computer program MINTEQA2 v. 1.50 (Allison et al., 1991). MINTEQA2 program uses built-in thermodynamic databases with the program itself (THERMO.DBS, TYPE6.DBS, REDOX.DBS, and GASES.DBS).

tial extraction results of 60 sediment samples collected from the entire depth profile (0—36.5 m) of monitoring wells showed that 20% total As (2—10 mg/kg) is complexed with amorphous Fe and Mn oxides in aquifer sediments. Arsenic abundance is not significant in exchangeable, carbonates or organic matter.

The results of chemical analyses showed that the organic matter content varied from below detection to 1% of the sediments. No reduced sulfur phases (e.g. pyrite or sediment sulfide) were detected in the sediments above the water table. But, significant reduced sulfur phases (below detection to 0.04%) were present in the sediments below the water table. Significant reduced sulfur phases were also present in sands at depth (10—36.6 m).

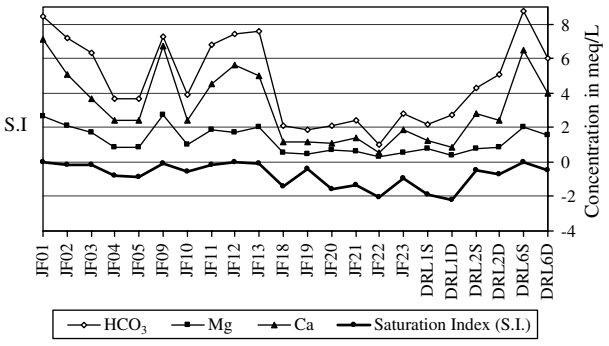

Figure 4 HCO_3^-, Ca^{2+}, Mg^{2+} increases as calcite approaches equilibrium due to the influence of the common ion effect.

General geochemical trends in groundwater

The groundwater in the area is generally of Ca^{2+}—HCO_3^- type (Fig. 3), with Ca^{2+} (10—143 mg/L) and HCO_3^- (63—533 mg/L). Water—rock interactions and associated chemical reactions (precipitation, dissolution, cation exchange, and adsorption) are responsible for the variation of chemical composition in groundwater. In the recharge area, the dominant geochemical process is the dissolution of carbonate minerals (e.g. calcite and dolomite), which contributes the Ca^{2+}, Mg^{2+}, and HCO_3^- to the groundwater. Chemical analysis of groundwater shows a general increase of Ca^{2+}, Mg^{2+}, alkalinity, pH, and TDS as the groundwater moves away from the recharge area (down gradient) which could be the result of calcite and dolomite dissolution. The concentration (meq/L) of $(Ca^{2+} + Mg^{2+})$ and $(HCO_3^- + SO_4^{2-})$ in groundwater samples show that both carbonate and silicate dissolution are present in the area. Groundwater in all the water-wells in the area is supersaturated with respect to silica. Localized gypsum dissolution along the flow path contributes both Ca^{2+} and SO_4^{2-} to groundwater. The Ca^{2+} released by the dissolution of gypsum leads to the precipitation of additional calcite and an increase in CO_2, which leads to a slightly low pH and supersaturation or near equilibrium of groundwater with calcite. This phenomenon is referred to as common-ion driven precipitation or common ion effect (Back and Hanshaw, 1970; Langmuir, 1997). The common ion effect of gypsum dissolution and calcite precipitation is often accompanied by dolomite dissolution, leading to the observed increase in Mg^{2+} (Fig. 4) in groundwater (JF1, JF2, JF3, JF9, JF11, JF12, JF13, and DRL6S). Gypsum is controlling Ca^{2+} solubility where SO_4^{2-} concentration is relatively high. Anaerobic decay of organic matter and SO_4^{2-} reduction (both reaction release CO_2) are controlling the SO_4^{2-} concentration in groundwater and subsequent increase in HCO_3^- and decrease in pH. HCO_3^- is always higher than equivalent Ca^{2+}, which is an indication that some HCO_3^- is also coming

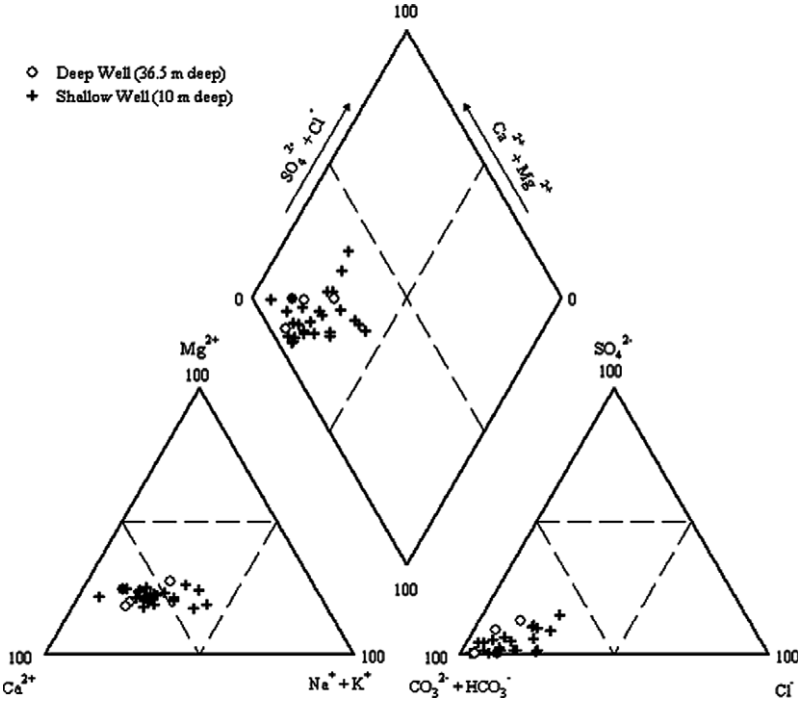

Figure 3 Piper's (1944) diagram of the geochemical evolution of groundwater in the area.

from processes other than calcite dissolution, or the Ca^{2+} is lost in the cation exchange reactions. Dissolution of silicate (albite) and oxidation of organic matter may have produced the excess HCO_3^- in the groundwater. The concentrations of Na^+ and Cl^- are relatively high away from the recharge area. An increase in Na^+/Cl^- ratios results in decreasing $(Ca^{2+} + Mg^{2+})/HCO_3^-$ ratios that are consistent with cation exchange along with high Na^+/Cl^- ratios. The concentrations (meq/L) of Na^+ and Cl^- in groundwater provide evidence that halite dissolution is not a major process controlling Na^+ and Cl^- in groundwater. Na^+ is comparatively higher than Cl^- in (more than half of all the irrigation wells) the majority of the wells, shows the evidence of silicate dissolution and cation exchange, rather than dissolution of halite (Kresse and Fazio, 2002). The Cl^- concentrations in the groundwater are relatively high (up to 116 mg/L) in the northeast and southeast portion of the study area, which may be the result of local recharge gained from surface contribution as recharge by river or irrigation return flow. There is a general decrease in ORP (measured as relative millivolt, RmV), DO, and NO_3^-N and a corresponding increase in NH_4—N along the flow path.

Hydrogeochemical data and the redox environment in the aquifer suggests reductive dissolution of Fe oxyhydroxide as the dominant As release mechanism. Calcite and gypsum solubility and simultaneous SO_4^{2-} reduction with co-precipitation of As and sulfide is an important limiting process controlling the concentration of dissolved As in groundwater. Spatial and temporal variability of As are controlled by spatial distribution of redox zones and the state of redox conditions, which depend on recharge potential, permeability of the upper aquitard, irrigation, and local flow dynamics in the aquifer. The redox state is the primary control on the rate of Fe oxyhydroxide reduction and the amount of As in groundwater.

Comparison of As geochemistry to alluvial aquifers in Bangladesh

Although the sediment As concentrations and groundwater chemistry in the alluvial aquifer of the Mississippi River Valley in southern Arkansas are similar to those in Bangladesh, the aqueous As concentrations in the research area (<0.5—77 μg/L) are generally far less than the values found in Bangladesh (2.5—846 μg/L; Ahmed et al., 2004). In Bangladesh, PO_4^{3-} concentrations (up to 8.75 mg/L; Swartz et al., 2004; Ahmed et al., 2004) in groundwater are very high compared to that in the research area (<0.1 mg/L). The most noticeable difference between the groundwater in Bangladesh and the research area is the concentration of SO_4^{2-} and its function relative to the reducing environment. Extensive SO_4^{2-} reduction has probably not occurred in Bangladesh, and thus As remained mobile in SO_4^{2-} reducing conditions (Zheng et al., 2004). One possible explanation for As to remain mobile in SO_4^{2-} reducing conditions in groundwater of Bangladesh is because there was insufficient initial SO_4^{2-} (<3 mg/L; Ahmed et al., 2004) to produce extensive SO_4^{2-} reduction, and authigenic sulfide precipitation to remove all the dissolved As (Zheng et al., 2004). On the contrary, in the research area within the Mississippi River Alluvial aquifer in Arkansas, SO_4^{2-} concentration varies from 1 to 46 mg/L, both spatially and vertically. At DRL6, SO_4^{2-} concentration is sharply reduced from 46 mg/L (DRL6S) to 1.4 mg/L (DRL6D), indicating extensive SO_4^{2-} reduction, and almost complete removal of dissolved As from 49.4 μg/L (DRL6S) to 1 μg/L (DRL6D). At DRL2, SO_4^{2-} behaves in the same way as in Bangladesh, where initial SO_4^{2-} concentration is very low (<1.5 mg/L) with relatively high As (>10 μg/L) at DRL2S. Insufficient initial SO_4^{2-} concentration at DRL2S leads to insignificant SO_4^{2-} reduction and sulfide precipitation, which ensures high dissolved As (>10 μg/L) at DRL2D. Aqueous As in Bangladesh is usually present as As^{3+} (67—99%; Ahmed et al., 2004). Dissolved S^{2-} (⩽2 mg/L; Broms and Fogelstörm, 2001) and NH_4^+ (up to 13.2 mg/L; Bhattacharya, 2002) are also present at relatively higher concentrations in Bangladesh. High concentration of biogenic CH_4^+ gas (>1% of CO_2 by volume) is reported in the groundwater in Bangladesh to be the byproduct of the microbial degradation of organic matter (Ahmed et al., 1998). Peat deposits are widespread and very common in the sedimentary sequence of alluvial aquifer in Bangladesh, which is considered as the potential redox driver for reductive dissolution of hydrous ferric oxides (HFO) (McArthur et al., 2004). Finally, the depositional environment of alluvial sediments in Bangladesh was different compared to the depositional history in the research area. The Ganges—Brahmaputra—Meghna River system transports huge amounts of sediment, and converge at the lower reaches (only several hundred kilometers from the source area) to form the great delta complex Ganges—Brahmaputra—Meghna (GBM) delta system. The deposited less reworked sediments are mostly immature with huge amounts of active organic matter (fermentation was incomplete) as the rate of deposition and successive burial was too fast to complete weathering processes (Brammer, 1996).

Interpretation of inverse modeling results

Potential phases in the inverse modeling were constrained (precipitation/dissolution) using compiled data of saturation indices derived from MINTEQA2 and a conceptual model inferred from general trends in chemical analyses data of groundwater. The inverse model was constrained so that primary mineral phases including quartz, calcite, dolomite, gypsum, halite, fluorite, ferrihydrite, and goethite were set to dissolve until they reached saturation, and siderite, FeS, and vivianite were set to precipitate once they reached saturation. Cation exchange reactions of Ca^{2+} for Na^+ on exchange sites were included in the model as a source for excess Na^+ in groundwater. Carbon dioxide and NH_4—N were assumed to be available throughout the flow path by incorporating reactions that produce oxidation of organic matter. Fe oxyhydroxide and SO_4^{2-} reduction by respiring microorganisms were considered to lead to sulfide precipitation. Kirk et al. (2004) reported that a mixed metabolic zone of microbial activity with variable rates of bacterial SO_4^{2-} reduction is controlling dissolved As in the alluvial aquifer in the Mahomet aquifer system, central Illinois, United States. The model also includes a H_2S gas phase due to the observation of H_2S odor during collection of groundwater samples, detection of dissolved S^{2-} in groundwater, and the presence of significant sulfide phases (<0.01—0.04% of sediment samples) in the sediments.

Table 7 Inverse modeling along the flow path JF21—JF10

Mineral phases	Phase state	Phase mole transfers JF23—JF10	Phase mole transfers JF21—JF10	Phase mole transfers JF19-JF10	Phase mole transfers JF13-JF10
Calcite	Dissolving	2.74E − 04	1.40E − 03	1.35E − 03	−
Gypsum	Dissolving	2.33E − 04	−	−	8.80E − 06
CH_2O	Dissolving	5.92E − 04	3.11	2.07	2.88
Halite	Dissolving	1.35E − 04	2.13E − 04	−	1.56E − 04
Fluorite	Dissolving	5.32E − 07	4.15E − 06	3.43E − 06	3.04E − 06
$Fe(OH)_3(a)$	Dissolving	1.79E − 04	1.25E + 01	8.29	−
FeS (ppt)	Precipitating	−2.72E − 04	−9.34	−7.68	−8.65
$H_2S(g)$	Dissolving	−	9.34	7.68	8.65
Siderite	Precipitating	−	−3.11	−6.12E − 01	−2.88
Sphalerite	Dissolving	−2.44E − 08	1.11E − 08	−	9.78E − 09
Barite	Dissolving	5.11E − 07	8.15E − 07	4.69E − 07	−2.03E − 07
Vivianite	Precipitating	−1.61E − 07	−2.64E-07	−7.09E − 07	−2.27E − 07
NaX	Dissolving		2.51E − 04	2.09E − 04	−
CaX_2	Precipitating	−2.27E − 04	−4.93E-04	−4.77E − 04	−
$CO_2(g)$	Precipitating	−	−	−1.46	−
$NH_3(g)$	Dissolving	6.43E − 06	−	−	−

Inverse model calculations were conducted using the computer program PHREEQC v. 2.13.0 (Parkhurst and Appelo, 1999). Thermodynamic database used: phreeqc.dat values are in mol/kg H_2O. Positive (mass entering water) and negative (mass leaving water) phase mole transfers indicate dissolution and precipitation, respectively.

Modeling results show that carbonates, gypsum, halite, fluorite, goethite, ferrihydrite, carbon dioxide (gas), and hydrogen sulfide (gas) are dissolving, whereas sphalerite, FeS, siderite, barite, and hematite are mostly precipitating along different flow paths in the groundwater system of the area. The Ca^{2+} released by the dissolution of gypsum leads to the precipitation of additional calcite, and an increase in CO_2, which leads to a slightly lower pH and supersaturation or near equilibrium of calcite. Cation exchange is contributing the relative abundance of Na^+ in groundwater. The groundwater is supersaturated with respect to quartz, hematite, magnetite, and pyrite based on saturation indices data from MINTEQA2. Siderite is precipitating in all the model runs, which is a limiting factor for Fe^{2+} in groundwater. The dissolution of Fe oxyhydroxide phases (e.g. ferrihydrite) is occurring in all the model runs, which is prerequisite for microbially mediated reductive dissolution of Fe oxyhydroxide as the releasing mechanism of As in groundwater. The precipitation of sulfide phases (e.g. sphalerite) along flow lines indicates the reduction of SO_4^{2-} and simultaneous precipitation of sulfide phases (e.g. sphalerite, FeS). The presence of significant amounts of dissolved S^{2-} and Fe^{2+} in groundwater and solid sediment sulfide in sediments indicates that SO_4^{2-} reduction and co-precipitation of sulfide and As might be an important geochemical process in the area. A mixed metabolic zone (Fe oxyhydroxide reducing bacteria, SO_4^{2-} reducing bacteria, and methanogens) of microbial activity may develop, where individual microbial activity may outcompete each other, or they may proceed simultaneously (Kirk et al., 2004). The relative rate of Fe oxyhydroxide reduction over SO_4^{2-} reduction with simultaneous co-precipitation of As as sulfide phases are the limiting factors controlling dissolved As in groundwater. The summary of the most optimum inverse model (JF21—JF10) for the selected simulations with phase mole transfers for the minerals and gases along the flow paths are given in Table 7.

Conclusions

The groundwater in the study area is characterized by the Ca^{2+}—HCO_3^- hydrochemical facies. Anions are dominantly composed of HCO_3^-. Cations are mostly composed of Ca^{2+} with a trend towards a localized increase in Na^+. Chemical analysis of groundwater shows a general increase in Ca^{2+}, Mg^{2+}, alkalinity, pH, and TDS as the groundwater moves away from the recharge area towards the discharge area (down gradient), which is the result of carbonate and silicate dissolution. Groundwater in all the irrigation and monitoring wells in the area is supersaturated with silica. The concentrations of $(Ca^{2+} + Mg^{2+})$ and $(HCO_3^- + SO_4^{2-})$ show that both carbonate and silicate dissolution occurs in the aquifer. Localized gypsum dissolution along the flow path contributes both Ca^{2+} and SO_4^{2-} to groundwater, which leads to a slightly low pH and supersaturation or near equilibrium of calcite due to the common ion effect. The common ion effect of gypsum dissolution and calcite precipitation is often accompanied by dolomite dissolution, which leads to the observed increase in Mg^{2+} in groundwater. Gypsum is controlling Ca^{2+} solubility where SO_4^{2-} concentration is relatively high. Calcite is generally near equilibrium where SO_4^{2-} is relatively high. The concentration of HCO_3^- in groundwater is always higher than equivalent amount of Ca^{2+}, which is an indication that either some HCO_3^- is also coming from processes other than carbonate dissolution, or some Ca^{2+} is lost in cation exchange reactions. Dissolution of silicate and oxidation of organic matter may have produced some HCO_3^- in the groundwater. Oxidation reduction potential and other redox sensitive chemical parameters show that the groundwater in the area falls in the mildly reducing (suboxic zone) to relatively highly reducing zone (anoxic zone). Hydrogeochemical data and redox environment in the area suggest microbially-mediated reductive dissolution of Fe oxyhydroxide as the dominant As release mechanism in

the area. Gypsum solubility and simultaneous SO_4^{2-} reduction with co-precipitation of As and sulfide is an important limiting process controlling the concentration of dissolved As in groundwater in the area.

The inverse geochemical modeling demonstrated that relatively few phases are required to derive the differences in groundwater chemistry along the flow path in the area. Inverse modeling suggests that dissolution of carbonate, gypsum, silica, and reductive dissolution of Fe oxyhydroxide and SO_4^{2-} mediated by oxidation of organic matter and microbial processes are the dominant geochemical processes in the area. Cation exchange of Ca^{2+} for Na^+ and precipitation of sulfide phases are also important geochemical processes in the aquifer system of the area. The inverse geochemical modeling supports the conceptualization of general hydrogeochemical processes gained from interpretation of general trends in the geochemical data. The model can incorporate the reductive dissolution of Fe oxyhydroxide as the dominant As release mechanism. Inverse modeling also demonstrates that gypsum solubility and simultaneous SO_4^{2-} reduction with co-precipitation of As and sulfide are important limiting processes controlling the concentration of dissolved As in groundwater.

References

Adeloju, S.B., Dhindsa, H.S., Tandon, R.K., 1994. Evaluation of some wet decomposition methods for mercury determination in biological and environmental materials by cold vapor atomic absorption spectroscopy. Anal. Chim. Acta 285, 359–364.

Ahmed, K.M., Bhattacharya, P., Hasan, M.A., Akhter, S.H., Alam, S.M.M., Bhuiyan, M.A.H., Imam, M.B., Khan, A.A., Sracek, O., 2004. Arsenic enrichment in groundwater of the alluvial aquifers in Bangladesh: an overview. Appl. Geochem. 19, 181–200.

Ahmed, K.M., Hoque, M., Hasan, M.K., Ravenscroft, P., Chowdhury, L.R., 1998. Origin and occurrence of water well methane gas in Bangladesh aquifers. J. Geol. Soc. India 51, 697–708.

Allison, J.D., Brown, D.S., Novo-Gradac, K.J., 1991. MINTEQA2/PRODEFA2, A Geochemical Assessment Model for Environmental Systems: Version 3.0 User's Manual. US Environmental Protection Agency, Athens, GA. EPA/600/3-91/021.

Apodaca, L.E., Jeffrey, B.B., Michelle, C.S., 2002. Water quality in shallow alluvial aquifers, Upper Colorado River Basin, Colorado, 1997. J. Am. Water Res. Assoc. 38 (1), 133–143.

Armienta, M.A., Villasenor, G., Rodriguez, R., Ongley, L.K., Mango, H., 2001. The role of arsenic-bearing rocks in groundwater pollution at Zimapan Valley, Mexico. Environ. Geol. 40, 571–581.

Back, W., Hanshaw, B.B., 1970. Comparison of chemical hydrology of Florida and Yucatan. J. Hydrol. 10, 360–368.

BGS and DPHE, 2001. Arsenic contamination of groundwater in Bangladesh. In: Kinniburgh, D.G., Smedley, P.L. (Eds.), British Geological Survey Report WC/00/19. British Geological Survey, Keyworth, UK.

Bhattacharya, P., 2002. Arsenic contaminated groundwater from the sedimentary aquifers of South-East Asia. In: Bocanegra, E., Martinez, D., Massone, H. (Eds.), Groundwater and Human Development, Proc. of the XXXII IAH and VI ALHSUD Congress, Mar del Plata, Argentina, 21–25 October 2002, pp. 357–363.

Bhattacharya, P., Welch, A.H., Ahmed, K.M., Jacks, G., Naidu, R., 2004. Arsenic in groundwater of sedimentary aquifers. Appl. Geochem. 19 (2), 163–167.

Brammer, H., 1996. The Geography of Soils of Bangladesh. University Press, Dhaka, Bangladesh.

Broms, S., Fogelstörm, J., 2001. Field investigations of arsenic-rich groundwater in the Bengal Delta Plain, Bangladesh. M.Sc. Thesis, Series 2001: 18, Department of Land and Water Resources Engineering, KTH, Stockholm.

Canfield, D.E., Raiswell, R., Westrich, J.T., Reaves, C.M., Berner, R.A., 1986. The use of chromium reduction in the analysis of reduced inorganic sulfur in sediments and shales. Chem. Geol. 54, 144–159.

Carrillo-Chavez, A., Drever, J.I., Martinez, M., 2000. Arsenic content and groundwater geochemistry of San Antonio-El Triunfo, Carrizal and Los Planes aquifers in southernmost Baja California, Mexico. Environ. Geol. 39, 1295–1303.

Chao, T.T., Zhou, L., 1983. Extraction techniques for selective dissolution of amorphous iron oxides from soils and sediments. J. Soil Sci. Soc. Am. 47, 225–232.

Charlton, S.R., Macklin, C.L., Parkhurst, D.D., 1997. PHREEQCI – a graphical user interface for the geochemical computer program PHREEQC. U.S. Geol. Survey Water Resources Investigation Report 97-4222.

Clark, A.K., Journey, C.A., 2006. Flow paths in the Edwards aquifer, northern Medina and northeastern Uvalde Counties, Texas, based on hydrologic identification and geochemical characterization and simulation. U.S. Department of the Interior, US Geol. Survey Scientific Investigation Report 2006-5200.

Clesceri, L.S., Greenberg, A.E., Eaton, A.D., 1999. Standard Methods for Examination of Water and Wastewater, 20th ed. American Public Health Association, Washington, DC.

Dai, Z., Samper, J., Ritzi Jr., R., 2006. Identifying geochemical processes by inverse modeling of multicomponent reactive transport in the Aquia aquifer. Geosphere 2 (4), 210–219.

Dhiman, S.D., Keshari, A.K., 2006. GIS assisted inverse geochemical modeling for plausible phase transfers in aquifers. Environ. Geol. 50, 1211–1219.

Dzombak, D.A., Morel, F.M.M., 1990. Surface Complexation Modeling: Hydrous Ferric Oxide. Willey, Toronto.

Eary, L.E., Runnels, D.D., Esposito, K.J., 2002. Geochemical controls on groundwater composition at the Cripple Creek Mining District, Colorado. Appl. Geochem. 18 (1), 1–24.

Edwards, M., Patel, S., McNeill, L., Chen, Hsiao-wen, Frey, M., Eaton, A.D., Antweiler, R.C., Taylor, H.E., 1998. Considerations in As analysis and speciation: a modified field technique can quantify particulate As, soluble As (III), and soluble As (V) in drinking water. J. AWWA 90 (3), 103–113.

Freiwald, D.A., 1985. Average annual precipitation and runoff for Arkansas, 1951–1980. U.S. Geological Survey Water Resources Investigation Report 84-4363, 1 sheet.

Grabinski, A.A., 1981. Determination of arsenic (III), arsenic (V), monomethylarsonate, and dimethylarsinate by ion-exchange chromatography with flameless atomic absorption spectrometric detection. Anal. Chem. 53, 966–968.

Guler, C., Thyne, G.D., 2002. Geochemical evolution of surface and groundwater in Indian Wells-Owens valley area and surrounding ranges, southeastern California, USA. GSA Abstracts with Programs 33 (4), A16.

Guler, C., Thyne, G.D., 2004. Hydrologic and geologic factors controlling surface and ground water chemistry in Indian Wells-Owens Valley area and surrounding ranges, California, USA. J. Hydrol. 285, 177–198.

Harvey, C.F., Ashfaque, K.N., Yu, W., Badruzzaman, A.B.M., Ali, M.A., Ostes, P.M., Michael, H.A., Neumann, R.B., Beckie, R., Islam, S., Ahmed, M.F., 2006. Groundwater dynamics and arsenic contamination in Bangladesh. Chem. Geol. 228, 112–136.

Hofmann-Wollenhof, B., Lichtenegger, H., Collins, J., 2001. GPS Theory and Practice, fifth ed. Springer Wien, New York.

Horneman, A., van Geen, A., Kent, D.V., Mathe, P.E., Zheng, Y., Dhar, R.K., O'Connell, S., Hoque, M.A., Aziz, Z., Shamsudduha, M., Seddique, A.A., Ahmed, K.M., 2004. Decoupling of As and Fe release to Bangladesh groundwater under reducing conditions. Part I: Evidence from sediment profiles. Geochim. Cosmochim. Acta 68 (17), 3459–3473.

Joseph, R.L., 1999. Status of water levels and selected water quality conditions in the Mississippi River Valley alluvial aquifer in eastern Arkansas. U.S. Geol. Survey Water Resources Investigation Report 99-4035, p. 54.

Kirk, M.F., Holm, T.R., Park, J., Jin, Q., Sanford, R.A., Fouke, B.W., Bethke, C.M., 2004. Bacterial sulfate reduction limits natural arsenic contamination of groundwater. Geology 32, 953–956.

Kleiss, B.A., Coupe, R.H., Gonthier, G.J., Justus, B.G., 2000. Water quality in the Mississippi Embayment, Mississippi, Louisiana, Arkansas, Missouri, Tennessee, and Kentucky, 1995–1998. U.S. Geol. Survey Circular 1208, 5–6.

Kresse, T.M., Fazio, J.A., 2002. Pesticides, Water quality and geochemical evolution of ground water in the alluvial aquifer, Bayou Bartholomew watershed, Arkansas. Arkansas Department of Environmental Quality. Water Quality Report WQ02-05-1, Little Rock, AR.

Kresse, T.M., Fazio, J.A., 2003. Occurrence of arsenic in groundwaters of Arkansas and implications for source and release mechanisms. Arkansas Department of Environmental Quality, Water Quality Report WQ03-03-01, Little Rock, AR.

Langmuir, D., 1997. Aqueous Environmental Geochemistry. Prentice-Hall, Upper Saddle River, NJ.

Lakshmanan, E., Kanan, R., Senthil Kumar, M., 2003. Major ion chemistry and identification of hydrogeochemical processes of groundwater in a part of Kancheepuram district, Tamil Nadu, India. Environ. Geos. 10 (4), 157–166.

Lecomte, K.L., Pasquini, A.I., Depetris, P.J., 2005. Mineral weathering in a semiarid mountain river: its assessment through PHREEQC inverse modeling. Aquatic Geochem. 11, 173–194.

McArthur, J.M., Ravenscroft, P., Safiullah, S., Thirlwall, M.F., 2001. Arsenic in groundwater: testing pollution mechanisms for sedimentary aquifers in Bangladesh. Water Res. Res. 37 (1), 109–117.

McArthur, J.M., Banerjee, D.M., Hudson-Edwards, K.A., Mishra, R., Purohito, R., Ravenscroft, P., Cronin, A., Howarth, R.J., Chatterjee, A., Talukder, T., Lowry, D., Houghton, S., Chadha, D.K., 2004. Natural organic matter in sedimentary basins and its relation to arsenic in anoxic groundwater: the example of West Bengal and its worldwide application. Appl. Geochem. 19, 1255–1293.

Miller, G.P., 2001. Surface complexation modeling of arsenic in natural water and sediment systems. Doctoral Dissertation, New Mexico Institute of Mining and Technology, New Mexico.

Miller, W.P., Miller, D.M., 1987. A micro-pipette method for soil mechanical analysis. Commun. Soil Sci. Plant Anal. 18 (1), 1–15.

Mirecki, J.E., 2006. Geochemical models of water-quality changes during aquifer storage recovery (ASR) cycle tests, Phase I: Geochemical models using existing data. ERDC/EL TR-06-8. U.S. Army Corps of Engineers, Engineering Research and Development Center, Vicksburg, MS, USA.

Nickson, R., McArthur, J.M., Ravencroft, P., Burgess, W.G., Ahmed, K.M., 2000. Mechanism of arsenic release to ground water, Bangladesh and West Bengal. Appl. Geochem. 15, 403–411.

Parkhurst, D.L., Appelo, C.A.J., 1999. User's guide to PHREEQC (ver.2) – a computer program for speciation, batch-reaction, one-dimensional transport, and inverse geochemical calculations. U.S. Geol. Survey Water Resources Investigation Report 99-4259.

Perry, E.F., 2001. Modeling rock–water interactions in flooded underground coal mines, Northern Appalachian Basin. Geochemistry: Explor. Environ. Anal. 1, 61–70.

Pfaff, J.D., 1993. Method 300.0: determination of inorganic anions in water by ion chromatography, Revision 2.1. US Environmental Protection Agency, Cincinnati, OH, USA.

Piper, A.M., 1944. A graphical interpretation of water analysis. Trans. Am. Geophys. Union 25, 914–928.

Plummer, L.N., Busby, J.F., Lee, R.W., Hanshaw, B.B., 1990. Geochemical modeling of Madison aquifer in parts of Montana, Wyoming, and South Dakota. Water Res. Res. 26 (9), 1981–2014.

Rodriguez, R.R., Basta, N.T., Casteel, S.W., Armstrong, F.P., Ward, D.C., 2003. Chemical extraction methods to assess bioavailable arsenic in soil and solid media. J. Environ. Qual. 32, 876–884.

Rosenthal, E., Jones, B.F., Weinberger, G., 1998. The chemical evolution of Kurnub Group paleowater in the Sinal-Negev province – a mass balance approach. Appl. Geochem. 13 (5), 553–569.

Savage, K.S., Bird, D.K., 2002. Inverse geochemical modeling of pit lake evolution in a high-arsenic, alkaline pit lake. GSA Abstr. Progr. 34, 51–52.

Schrader, T.P., 2001. Status of water levels and selected water quality conditions in the Mississippi River Alluvial aquifer in eastern Arkansas, 2000. U.S. Geol. Survey Water Resources Investigation Report 01-4124, p. 5.

Schreiber, J.A., Simo, J.A., Freiberg, P.G., 2000. Stratigraphic and geochemical controls on naturally occurring arsenic in groundwater, eastern Wisconsin, USA. Hydrogeol. J. 8, 161–176.

Sharif, M.U., 2007. Hydrochemical evolution of arsenic in groundwater: Sources and sinks in the Mississippi River Valley Alluvial aquifer, southeastern Arkansas, USA. Doctoral Dissertation, University of Arkansas, Arkansas, USA.

Shelton, L.R., Chapel, P.D., 1994. Guidelines for collecting and processing samples of stream bed sediment for analysis of trace elements and organic contaminants for the National Water-Quality Assessment (NAWQA) Program. USGS Open File Report 94-458.

Smedley, P.L., Kinniburgh, D.G., 2002. A review of the source, behavior and distribution of arsenic in natural waters. Appl. Geochem. 17, 517–568.

Smith, A.H., Lingas, E.O., Rahman, M., 2000. Contamination of drinking-water by arsenic in Bangladesh: a public health emergency. Bull. WHO 78, 1093–1103.

Sracek, O., Bhattacharya, P., Jacks, G., Gustafsson, J., Bromssen, M., 2004. Behavior of arsenic and geochemical modeling of arsenic enrichment in aqueous environments. Appl. Geochem. 19, 169–180.

Swartz, C.H., Keon, N.E., Badruzzaman, B., Ali, A., Brabender, D., Jay, J., Besancon, J., Islam, S., Hemond, H.F., Harvey, C.F., 2004. Mobility of arsenic in Bangladesh aquifer: inferences from geochemical profiles, leaching data, and mineralogical characterization. Geochim. Cosmochim. Acta 68 (22), 4539–4557.

Tessier, A., Campbell, P.G.C., Bisson, M., 1979. Sequential extraction procedure for the speciation of particulate trace metals. Anal. Chem. 51 (7), 844–851.

US Environmental Protection Agency, 1994. Analytical methods manuals – methods for the determination of metals in environmental samples, Supplement I, EPA/600/R-94/111, EPA, Cincinnati, OH, USA.

US Environmental Protection Agency, 1999. EPA method 21: determination of volatile organic compounds leaks. Code of Federal Regulations 40, part 60, revised July, 1999, EPA, Cincinnati, OH, USA.

Wayne, W.L., Franceska, D.W., Michael T.K., 1997. Guidelines and standard procedures for studies of ground-water quality: Selection and installation of wells, and supporting documentation. U.S. Geological Survey Water Resources Investigation Report 96-4233.

Zheng, Y., Stute, M., Van Geen, A., Gavrieli, I., Dhar, R., Simpson, H.J., Schlosser, P., Ahmed, K.M., 2004. Redox control of arsenic mobilization in Bangladesh groundwater. Appl. Geochem. 19, 201–214.

Zheng, Y., van Geen, A., Stute, M., Dhar, R., Mo, Z., Cheng, Z., Horneman, A., Gavrieli, I., Simpson, H.J., Versteeg, R., Steckler, M., Grazioli-Venier, A., Goodbred, S., Shahnewaz, M., Shamsudduha, M., Hoque, M.A., Ahmed, K.M., 2005. Geochemical and hydrogeological contrasts between shallow and deeper aquifers in two villages of Araihazar, Bangladesh: implications for deeper aquifers as drinking water sources. Geochim. Cosmochim. Acta 69 (22), 5203–5218.

Zhu, C., Anderson, G., 2002. Environmental Application of Geochemical Modeling. Cambridge University Press, Cambridge.